Airfoil Modeling

Paul Nadan, Sean Szymanski, Colvin Chapman

May 2018

1 Introduction to Aerodynamics and Airfoils

The performance of an airfoil is primarily determined by its effect on the fluid particles around it. The fluid - which is naturally made up of discrete particles - is abstracted to a continuum with each point in space-time corresponding to an infinitely small particle with a finite density, and velocity.

These interactions between the airfoils and the air generate lift, the component of force in the vertical direction, and drag, the component of force in the horizontal direction. The shape, size, angle of attack, camber and other parameters can affect the amount of lift and drag that the airfoil produces. Measuring and modeling these forces is an incredibly complex, yet important task in studying airborne objects. There are many different ways to model airfoils, each with varying degrees of complexity. We took a deeper dive into one of the models, using Laplace's Equation and Joukowski Transforms, to see if we could better understand and model the function of an airfoil.

2 Laplace's Equation

With the significant, somewhat simplistic assumptions of irrotational, incompressible, inviscid, two-dimensional flow, we can reduce our fluid model to a more tractable form.

2.1 Velocity Potential

The irrotational condition indicates that the curl of the velocity is zero at every point. The velocity is thus a conservative vector field, which allows us to define a velocity potential, Φ, whose gradient is the velocity field. Laplace's equation (Equation 1) then arises from the "incompressible" assumption, which simply states that the divergence of the velocity field must be zero. If this quantity were nonzero, the velocity vectors would be either be diverging or converging, meaning the fluid would be expanding or compressing.

$$\nabla^2\Phi(x,y) = 0 \tag{1}$$

By definition, the velocity at any given point will flow in the direction of the gradient of the the velocity potential Φ. Satisfying the Cauchy-Riemann equations (Equations 2 and 3), the stream function Ψ has a gradient orthogonal to $\nabla\Phi$. This means that the contours of Ψ are the streamlines of the fluid around the object - the paths that individual fluid particles could take.

$$\frac{\partial\Phi}{\partial x} = \frac{\partial\Psi}{\partial y} \tag{2}$$

$$\frac{\partial\Psi}{\partial x} = -\frac{\partial\Phi}{\partial y} \tag{3}$$

A special particular solution to Laplace's equation is a doublet: $\frac{V_\infty R^2 x}{x^2+y^2}$. This is especially interesting since its contours - and more importantly,the contours of the corresponding stream function - make circles. This is very useful for modeling flow across a cylinder, since we know that the streamlines at the boundary of the surface will trace an outline of the surface. The only exception is that there is no velocity in the "dead zones", which are the two points without any velocity where the streamlines split at the front (so some can go above and others below the object) and come together at the back. To be complete, we have to add the doublet to a free stream ($V_\infty x$) and a point vortex ($\frac{\Gamma}{2\pi tan^{-1}(\frac{y}{x})}$). (Where V_∞ represents the speed of the stream far away from the object in question, and Γ represents the circulation around the surface of the object).

$$\Phi(x,y) = V_\infty x + \frac{V_\infty R^2 x}{x^2+y^2} + \frac{\Gamma}{2\pi tan^{-1}(\frac{y}{x})} \tag{4}$$

$$\Psi(x,y) = V_\infty y - \frac{V_\infty R^2 y}{x^2+y^2} - \frac{\Gamma}{4\pi ln(x^2+y^2)} \tag{5}$$

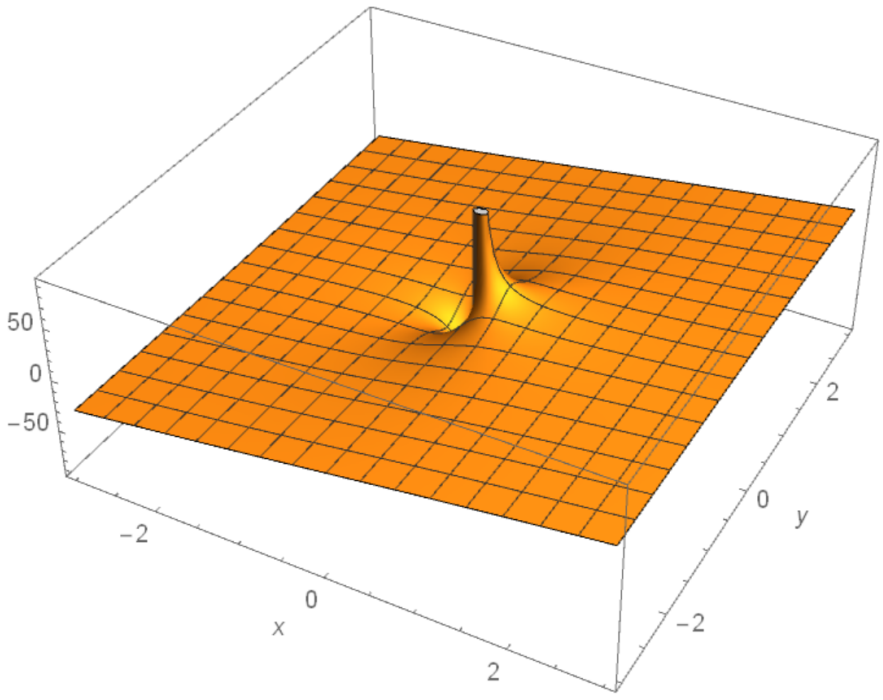

Figure 1: A 3D Visualization of the velocity potential of airflow around a unit cylinder without circulation. The free stream flowing in positive x takes the form of a plane sloping positively in x.

2.2 Velocity Vector Flow

An important step in the process to understanding the response of the fluid flow to the object is the solving for the velocity vector function. Equations 7 and 8 calculate the respective x and y components of the velocity vector ($\vec{U}$). The computed velocity field around a cylinder is visualized in Figure 2.

$$\vec{U}(x,y) = [u(x,y), v(x,y)] \tag{6}$$

$$u(x,y) = \frac{\partial \Phi(x,y)}{\partial x} = V_\infty + V_\infty R^2 \frac{y^2 - x^2}{(x^2+y^2)^2} - \frac{\Gamma}{2\pi}\frac{y}{x^2+y^2} \tag{7}$$

$$v(x,y) = \frac{\partial \Phi(x,y)}{\partial y} = -2V_\infty R^2 \frac{xy}{(x^2+y^2)^2} + \frac{\Gamma}{2\pi}\frac{x}{x^2+y^2} \tag{8}$$

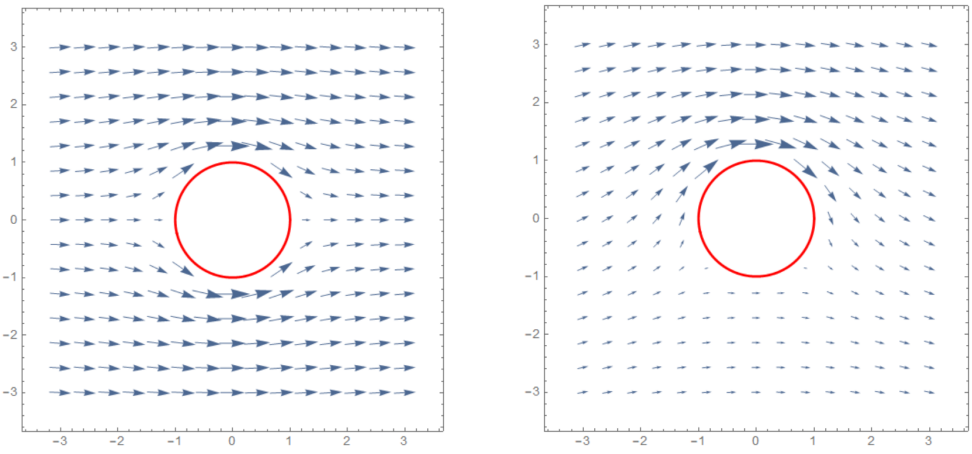

(a) Without Circulation

(b) With Circulation $\Gamma = -8$

Figure 2: Velocity vector field around a cylinder cross section. The horizontal axis is x, and the vertical is y.

2.3 Pressure Field

One of our modeling assumptions is that the fluid is incompressible. However, we can still find an estimate of the relative pressure $p(x,y)$ using the magnitude of the velocity at a specific point. Bernoulli's equation tells us energy is conserved through time (Equation 9). Since each particle enters at the same speed and pressure in the constant flow, the constant c will be the same everywhere. We defined the pressure in the free stream to be zero, since we are interested in the pressure relative to the free stream. The pressure relative to the free stream is calculated in Equation 10. Any change in the $\frac{\rho|u|^2}{2}$ term has to be balanced by the p to keep c constant. Figure 3 shows a 3D visualization of pressure where the height of the surface corresponds to the relative pressure at that x and y position.

$$p + \frac{\rho|u|^2}{2} = c \tag{9}$$

$$p(x,y) = \frac{\rho U^2}{2} - \frac{\rho|u|^2}{2} \tag{10}$$

2.4 Lift and Drag

Now for the fun stuff! When designing an airfoil, the factors you really care about are the macroscopic forces applied to the airfoil by the fluid. This is computed by finding the vector normal to the surface of the airfoil with a magnitude equal to the pressure ($p\hat{n}$), and integrating around the perimeter of the airfoil.

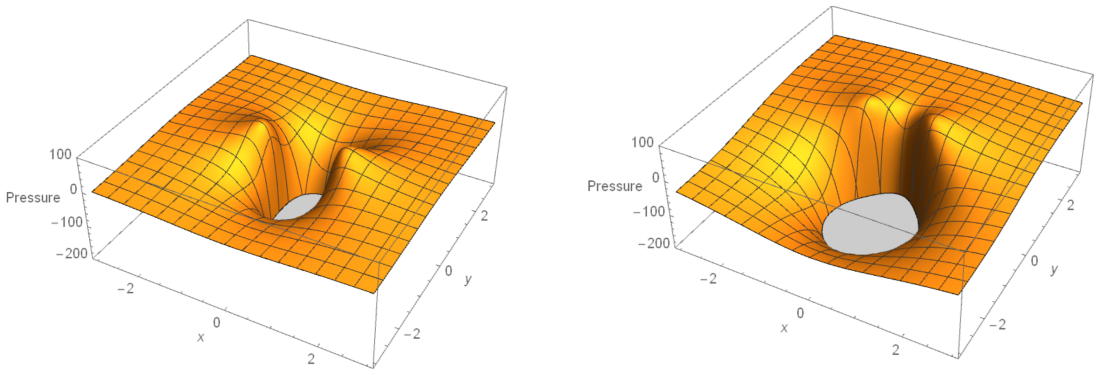

(a) Without Circulation

(b) With Circulation $\Gamma = 8$

Figure 3: Pressure distribution of airflow across a cylinder.

$$F_{drag} = \int_{circle} p(\vec{r})\hat{n}_x(\vec{r})d\vec{r} = -\int_0^{2\pi} p(Rcos(\theta), Rsin(\theta))cos(\theta)Rd\theta \tag{11}$$

$$F_{lift} = \int_{circle} p(\vec{r})\hat{n}_y(\vec{r})d\vec{r} = -\int_0^{2\pi} p(Rcos(\theta), Rsin(\theta))sin(\theta)Rd\theta \tag{12}$$

3 Joukowski Transform

While it is relatively straightforward to find the potential function for flow around a cylinder, an additional technique is needed to model more complicated surfaces, like airfoils. The Joukowski transform is a conformal mapping that transforms a circle in the complex plane into a more airfoil-like shape, while also transforming the velocity vector field in a way that still satisfies Laplace's equation.

3.1 Creating Joukowski Airfoils

The Joukowski transform requires a complex variable input, so the circle in the x-y plane must first be expressed as a single complex variable (ζ) according to Equation 13. The Joukowski transform of the circle can then be computed using Equation 14.

$$\zeta = x + iy = Rcos(\theta) + iRsin(\theta) + x_0 + iy_0 = Re^{i\theta} + \zeta_0 \tag{13}$$

$$z = \zeta + 1/\zeta \tag{14}$$

Through trial and error, we found a set of parameters for the midpoint ($\zeta_0 = -0.22 + 0.125i$) and radius (R=1.25) of the original circle that produced a nice-looking airfoil shape (Figure 4).

3.2 Complex Potential

A complex potential can be defined from the potential and stream functions as $\Omega = \Phi + \Psi$. A complex function is differentiable if and only if its real and complex components satisfy the Cauchy-Riemann equations (Equations 2 and 3), which imply that the function also satisfies Laplace's equation (Equation 1). Both the complex potential Ω and the Joukowski transform z satisfy the Cauchy-Riemann equations, thus they are both complex differentiable. If two functions f and g are complex differentiable, then so is their composition $f(g)$. Therefore, the composition of the complex potential Ω and the Joukowski transform z is also complex differentiable, and provides a valid solution to Laplace's equation.

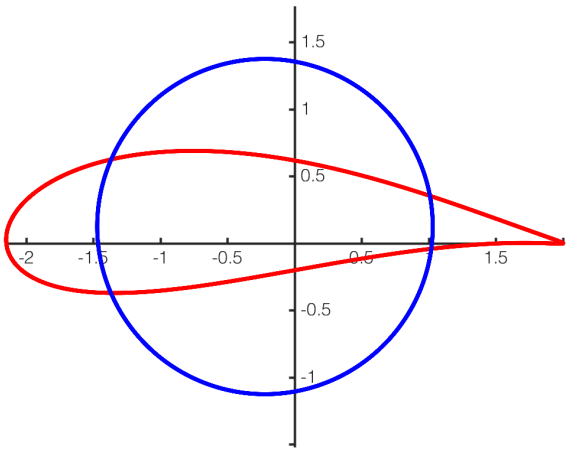

Figure 4: A circle (blue) and its Joukowski transform (red), overlaid in the complex plane.

3.3 Velocity Vector Flow

By substituting $\zeta = x + iy$ into the velocity vector field equations given above (Equation 7 and 8) and simplifying algebraically, we can define a complex velocity vector field for flow around the circle $\widetilde{W} = u + iv$ (Equation 15). Note the addition of an $e^{-i\alpha}$ term; α is the angle of attack, so $e^{-i\alpha}$ represents a rotation of the incoming air stream (it's simpler to just rotate the oncoming wind than to rotate the airfoil itself).

$$\widetilde{W}(\zeta) = V_\infty e^{-i\alpha} - \frac{V_\infty R^2 e^{i\alpha}}{(\zeta - \zeta_0)^2} - \frac{i\Gamma}{2\pi(\zeta - \zeta_0)} \tag{15}$$

Given that the velocity vector field is the gradient of the potential function, we can then apply the chain rule to find the velocity vector field for the transformed airfoil, W (Equation 16).

$$W(z) = \widetilde{W}(\zeta)\frac{d\zeta}{dz} = \frac{\widetilde{W}(\zeta)}{1 - \frac{1}{\zeta^2}} \tag{16}$$

Using MATLAB, we computed the velocity field around our airfoil, shown in Figure 5.

3.4 Kutta Condition

For the case of flow around a cylinder, we were free to set the circulation Γ to any value we chose. However, for our Joukowski airfoil, the circulation must be chosen to satisfy the Kutta condition. In order for air to flow around the sharp tail of the airfoil, it would have to undergo impossibly high acceleration. This problem is avoided, however, if the tail velocity is zero. By changing the circulation value, we can move the dead spots (points of zero velocity) around the boundary of the airfoil until one of them rests at the tail, satisfying the Kutta condition. The Joukowski transform has the property that the x-intercepts of the original circle map to the tip and tail of the airfoil. By setting the velocity at the x-intercept to zero, we can solve for the value of the circulation in terms of the angle of attack (Equation 18). β is defined as the angle from the center of the untransformed circle to the x-axis.

$$\beta = sin^{-1}(\frac{y_0}{R}) \tag{17}$$

$$\Gamma = -4\pi R sin(\alpha + \beta); \tag{18}$$

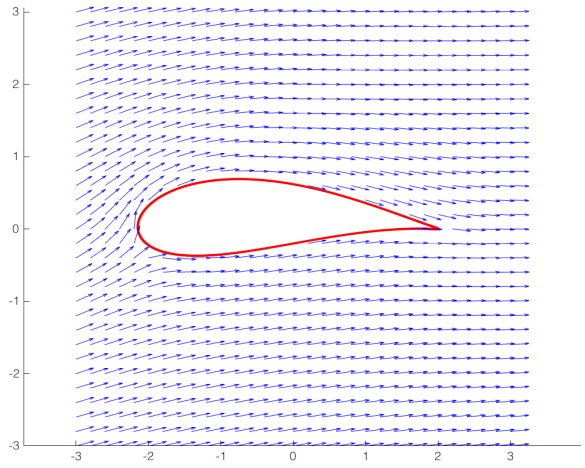

Figure 5: The velocity vector field around a Joukowski airfoil with a 10 degree angle of attack.

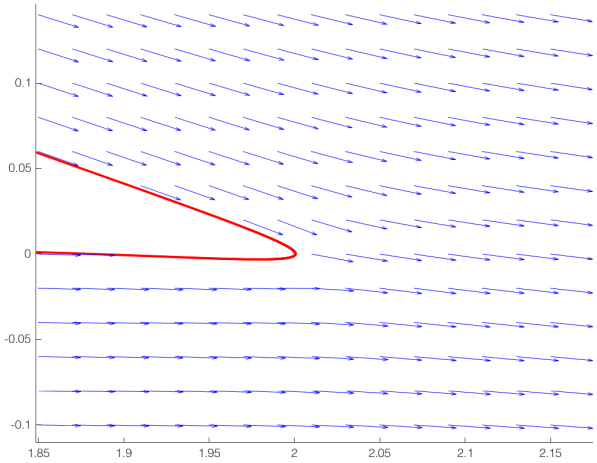

Figure 6: The tail of an airfoil with the Kutta condition satsfied. Notice how the velocity vectors leaving the tail from either side merge seamlessly.

3.5 Lift and Drag of a Joukowski Airfoil

Now that we have found our complex velocity vector field, we can calculate the pressure using Equation 10 above. By integrating the horizontal and vertical components of the pressure force around the boundary of the transformed airfoil, we can compute the net drag and lift respectively that the airfoil will experience (Equation 19 and 20).

$$F_{drag} = \int_{airfoil} p(\vec{r})\hat{n}_x(\vec{r})d\vec{r} = -\int_0^{2\pi} p(z(\theta))im(\frac{\partial z}{\partial \theta})d\theta \tag{19}$$

$$F_{lift} = \int_{airfoil} p(\vec{r})\hat{n}_y(\vec{r})d\vec{r} = \int_0^{2\pi} p(z(\theta))re(\frac{\partial z}{\partial \theta})d\theta \tag{20}$$

A sample result is shown for the Joukowski airfoil at a 10 degree angle of attack (Figure 8).

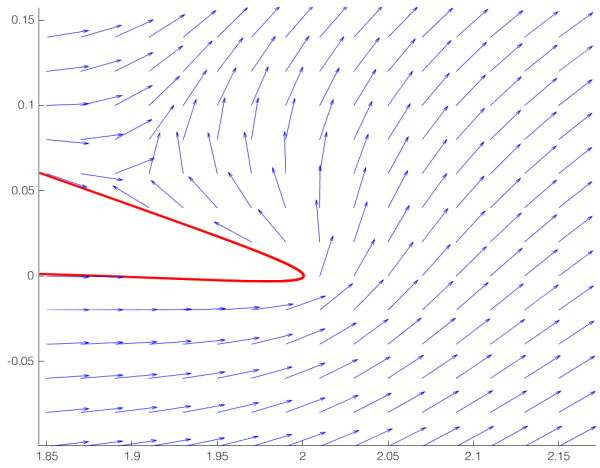

Figure 7: The tail of an airfoil with the Kutta condition not satisfied. The dead spot occurs on the top side of the airfoil, forcing air to flow around the tail.

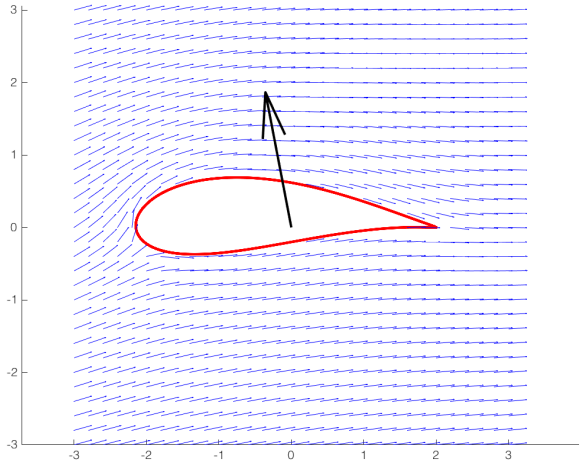

Figure 8: The net force vector applied to a Joukowski airfoil with a ten degree angle of attack. The magnitude was rescaled to better fit the image, but the direction reveals the ratio between the lift and drag. Note that the coordinate system is rotated such that the x-axis is parallel to the airfoil, rather than the oncoming air stream.

4 Finite Element Analysis of Airfoils

After implementing our own version of the model, we decided to input the same model components into a more reliable fluid simulator to help us gain more insight into the true behavior of flow around an airfoil. We chose to model both a simple cylinder and a Joukowski airfoil with a flow simulation in SolidWorks to do this.

4.1 Simple Cylinder

For this simulation, a cylinder was generated with a radius of 1 meter and a thickness of 1 meter. It was subjected to a 1 m/s wind in the x direction.

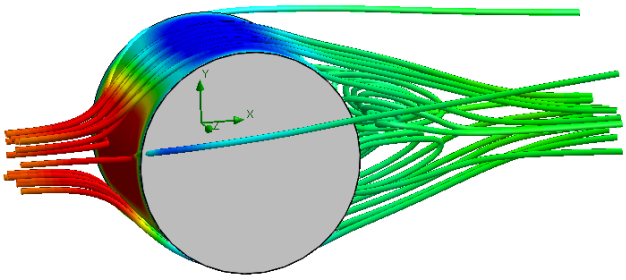

Figure 9: Aerodynamic Simulation of a Simple Cylinder.

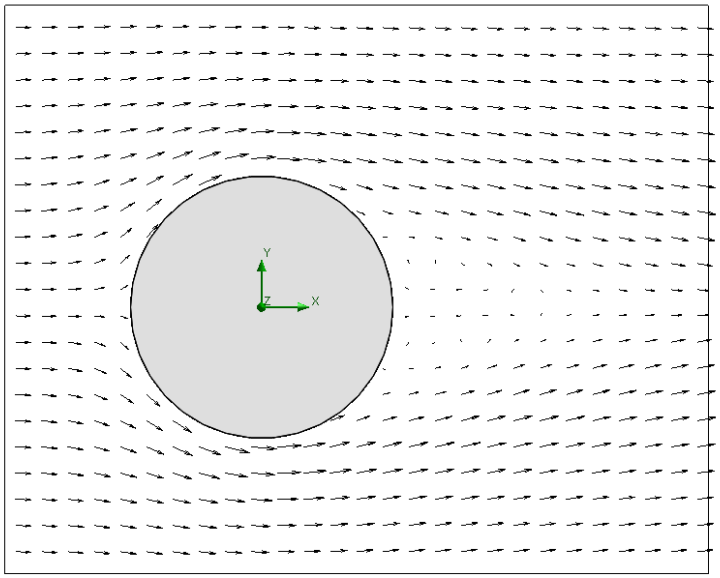

Figure 10: Vector Plot for Aerodynamic Simulation of a Simple Cylinder.

The result of this simulation was as expected. The front of the cylinder experiences a high pressure zone where the wind hits the cylinder head on. The cylinder also experiences a dead spot at the top and bottom of the cylinder. Both of these things existed in our mathematica model. However, this model differs in the back of the cylinder. There, it has a turbulent flow, as one might expect in real life. Due to the fact that our model assumes an irrotational flow, we do not see this in our model. The model experiences a drag force of 0.403 N and a lift force of -0.00396 N. According to our simplified model, both lift and drag on the cylinder should be zero. However, the nonzero drag force arises from the viscous forces present in our FEA simulation but neglected by our assumption of inviscid flow.

4.2 Joukowski Airfoil

For this simulation, we used the resulting parametric equations for a Joukowski transform that we calculated in Mathematica to create a Solidworks sketch. The equations that define the Joukowski transform are:

$$X(x_0, y_0, R) = x_0 + Rcos(t) + \frac{x_0}{(x_0 + Rcos(t))^2 + (y_0 + Rsin(t))^2} + \frac{Rcos(t)}{(x_0 + Rcos(t))^2 + (y_0 + Rsin(t))^2)} \quad (21)$$

$$Y(x_0, y_0, R) = y_0 + Rsin(t) - \frac{y_0}{(x_0 + Rcos(t))^2 + (y_0 + Rsin(t))^2} - \frac{Rsin(t)}{(x_0 + Rcos(t))^2 + (y_0 + Rsin(t))^2} \quad (22)$$

On the interval: $0 \leq t \leq 2\pi$

Specifically, we used the coefficients $y_0 = .125$m, $x_0 = -.22$m, and $R = 1.25$m, which were chosen to match the airfoil that we created to test our Mathematica and MATLAB code. After creating the sketch, we extruded it to a depth of 1 meter to match the model. Then, we then ran two SolidWorks flow simulations of this airfoil with a windspeed of 1 m/s and an angle of attack of 0°and 10°.

4.3 Joukowski Airfoil with 0° Angle of Attack

The 0°angle of attack was achieved by running the simulation with a 1m/s wind solely in the x-direction.

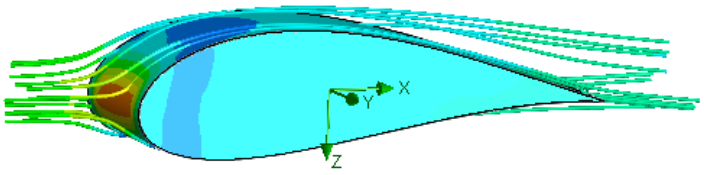

Figure 11: Aerodynamic Simulation of a Joukowski Airfoil.

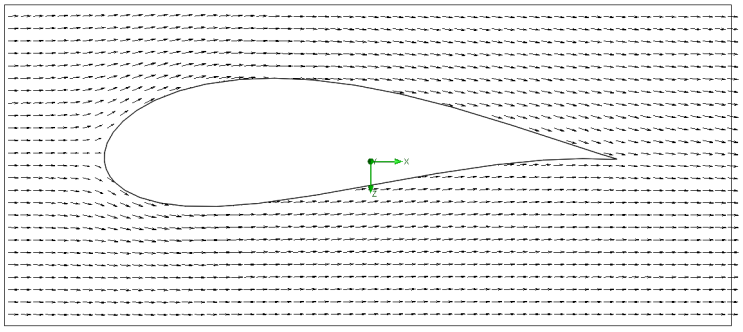

Figure 12: Vector Plot Aerodynamic Simulation of a Joukowski Airfoil.

This simulation resulted in output as expected. The model had a high pressure spot at the top of the airfoil and a low pressure spot on the upper side of the airfoil. The vector plot shows the streamlines meeting at the end of the airfoil, showing that the airfoil satisfies the Kutta conditions. This model also gave values of drag for this airfoil as 0.194 N and the lift as 0.00513 N. We expect the drag to be nonzero for this model, as the air is hitting it horizontally. However, we expect the lift to be 0 for a horizontal wind on a Joukouwski airfoil with no circulation. The simulation successfully validates these expectations.

4.4 Joukowski Airfoil with 10°Angle of Attack

In order to create a 10°angle of attack, we determined the components of wind speed which would create a 10°angle while still maintaining a 1 m/s wind overall. Those components are .985 m/s in the x-direction and .174 m/s in the y direction. We then ran the simulation with these components.

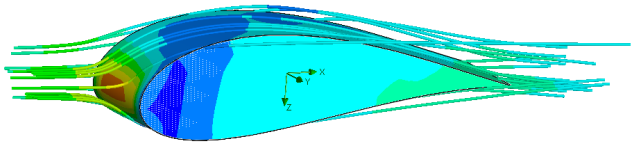

Figure 13: Flow Lines of a Joukowski Transform with a 10°Angle of Attack.

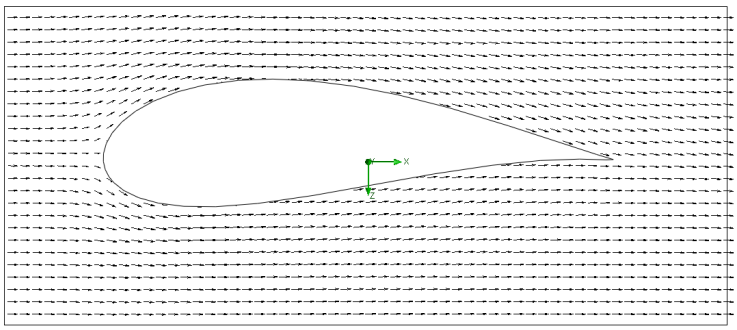

Figure 14: Vector Field of a Joukowski Airfoil with a 10°Angle of Attack.

The simulation also looked as expected with a 10°angle of attack. There was still the high pressure area up front, but it was shifted lower than on the airfoil with no angle of attack. This shift is due to the angle of attack changing which surface of the airfoil hits the wind head-on. In addition, the dead spot on the top of the airfoil shifted forward and became larger, again due to the angle of attack. Finally, the vector field shows that the streamlines still meet at the tail of the airfoil, therefore satisfying the Kutta conditions. The simulations gave us a value for drag of 0.217 N and lift of 0.224 N. The lift of this airfoil is dramatically larger than the lift of the airfoil with a 0 degree angle of attack, which is as we would expect.

5 Conclusion

While we were unable to numerically match our mathematical results to those of flow simulations in SolidWorks, we still obtained some very convincing results. Our airfoil model acts as one would expect, generating high pressure spots in the front and low pressure points away from the front. It also satisfies the Kutta condition and can successfully implement an angle of attack. There are still many more complex

fluid models out there to master, but we have successfully taken the first steps towards understanding and modeling complex aerodynamic systems.

References

[1] A.H. Techet *"Potential Flow Theory", 2.016 Hydrodynamics,* http://web.mit.edu/2.016/www/handouts/2005Reading4.pdf.

[2] E.L. Houghton, P.W. Carpenter, Steven H. Collicott, Daniel T. Valentine Aerodynamics for Engineering Students. *Sixth Edition*, http://rahauav.com/Library/Aerodynamic/Aerodynamics%20for%20engineering%20students_6th_www.rahauav.com.pdf.

[3] *"Joukowski Mapping:Topic 16"*, http://www2.esm.vt.edu/~dtmook/AOE5104_ONLINE/Class%20Notes/16_Class_JoukowskiMapping.pdf.

[4] Nitin R. Kapania, Katherine Terracciano, Shannon Taylor *"Modeling the Fluid Flow around Airfoils Using Conformal Mapping, Siam.org", 29 Aug. 2008,* https://www.siam.org/students/siuro/vol1issue2/S01010.pdf.

[5] Vermont Veterinary and Cardiology Services *Velocity and Pressure Distribution for Flow Over a Cylinder],* http://www.vermontveterinarycardiology.com/index.php/for-cardiologists/for-cardiologists?id=127.